Journal of
Composites Science

MDPI

Review

A Review on Analysis of Reinforced Recycled Rubber Composites

Gamze Cakir Kabakçi [1,2], Ozgur Aslan [2] and Emin Bayraktar [1,*]

[1] School of Mechanical and Manufacturing Engineering, ISAE-Supmeca-Paris, Saint Ouen, 93407 Paris, France
[2] Department of Mechanical Engineering, Atilim University, Incek Golbasi, Ankara 06830, Turkey
* Correspondence: emin.bayraktar@isae-supmeca.fr; Tel.: +33-6-76-10-36-20

Abstract: Rubber recycling attracts considerable attention by a variety of industries around the world due to shrinking resources, increasing cost of raw materials, growing awareness of sustainable development, and environmental issues. Recycled rubber is commonly used in aeronautic, automotive, and transportation industries. In this study, recycled rubber composites designed with different reinforcements in the literature are scrutinized by means of toughening mechanisms, mechanical and physical properties, as well as microstructural and fracture surface analysis. Microscale reinforcements (glass bubbles, alumina fiber, etc.) and nanoscale reinforcements (nanosilica, graphene nanoplatelets, etc.) utilized as reinforcements in rubber composites are thoroughly reviewed. The general mechanical properties reported by previous studies, such as tensile, compressive, and flexural strength, are investigated with the main goal of optimizing the amount of reinforcement used. The majority of the studies on recycled rubber composites show that recycled rubber reinforced with microscale particles leads to the development of physical and mechanical properties of the structures and also provides low-cost and lightweight composites for several application areas. Moreover, recycled rubber containing composites can be suitable for applications where high toughness and high resistance to impact are desirable. The present review aims to demonstrate research on reinforced recycled rubber composites in the literature and prospective outcomes.

Keywords: recycled rubber composites; microscale reinforcements; toughening mechanisms; fracture surface analysis

Citation: Kabakçi, G.C.; Aslan, O.; Bayraktar, E. A Review on Analysis of Reinforced Recycled Rubber Composites. *J. Compos. Sci.* **2022**, *6*, 225. https://doi.org/10.3390/jcs6080225

Academic Editor: Francesco Tornabene

Received: 29 June 2022
Accepted: 1 August 2022
Published: 4 August 2022

1. Introduction

Due to limited resources and increasing raw material costs, recycling of rubber has gained importance across numerous industries including transportation, automotive, and aerospace [1,2]. For instance, reduction of overall cost and mass reduction to lower fuel consumption and CO_2 emissions of an aircraft are desirable by aeronautic companies. Therefore, development of low-cost and lightweight materials for use in manufacturing constitutes an important goal.

In various industries, such as sportive equipment and flexible tube manufacturing for automotive and aeronautic industries, waste rubbers are produced and referred to as factory wastes, which take part of 5–15% of total output. Few examples of common rubber manufacturing processes that result in scrap rubber can be provided. For example, 20–40% of the rubber is wasted during the stamping out of gaskets from cured sheet rubber. Furthermore, 30–50% of the rubber is wasted during the injection molding process, which is used to prepare molded composites by injecting polymer resin mixing with a hardener and a catalyst, then transferring under pressure and solidifying them [3,4]. Thereafter, the extrusion process which turns rubber materials into a specifically shaped product makes rubber-based goods result in 2–5% of rubber waste [5]. In addition, the scrap rubber discarded right after the production line is used as a fossil fuel in a variety of applications, including cement kilns, paper mills, and power plants. On the other hand, the ecosystem is harmed by energy recovery from scrap rubber. Following this step, the non-use of

these recycled rubbers is considered a financial loss. Therefore, it is critical to establish cost-effective methods for recycling scrap rubbers.

Almost all of the rubber products are properly crosslinked to achieve the desired properties of elasticity, resilience, tensile strength, viscosity, and hardness. As a result, at high temperatures, vulcanized rubber products do not become liquid and cannot be easily reprocessed into a different form. Therefore, the disposal of used or scrap rubber has been a technical, ecological, and economic issue for production and use [6]. For example, non-used vulcanized scrap rubber that has strong bonds and the specific composition including sulfur [5] occupies large amounts of landfill space. In addition, it holds water for a long amount of time and this creates a habitat for mosquito larvae, rodents, and snakes that carry infections, such as malaria, cephalitis, dengue, etc. [6]. Moreover, if these rubber piles burst into flames, it is difficult to extinguish them [7]. Finally, some additives found in landfilled end-of-life rubbers, such as colorants, stabilizers, flame retardants, and plasticizers, can leach into the soil and these additives have the potential to destroy beneficial bacterial colonies in the soil [3,8]. As a result, vulcanized rubber recycling is a hot topic, with several countries putting in place necessary measures [9].

Vulcanization is a chemical process in which the rubber is heated with sulphur, accelerator, and activator at 140–160 °C. The process involves the formation of crosslinks between long rubber molecules [6–11]. The vulcanization process is necessary to produce most useful rubber articles, such as tires and mechanical goods. Unvulcanized rubber is generally not strong, and does not retract essentially to its original shape after a large deformation [3]. Once the rubber is crosslinked, it is difficult to recycle. Devulcanization of cured rubber ensures the reversion of the crosslinking process, which leads to obtaining recycled material with properties very close to the original material [10–12]. It is also realized to improve the interaction and adhesion between recycled rubber and matrix. The devulcanization is a technique that causes the selective fracture of sulfur-sulfur (S–S) and carbon-sulfur (C–S) chemical bonds without causing the backbone network to break or the material to degrade. During the devulcanization process, sulphur links are tried to be broken and new other links are generated, then the flowing capacity and interaction of recycled rubbers with other substances are increased.

Rubber is commonly utilized in industry due to its effective energy absorption capability. Compared to other materials, it can be deformed considerably more elastically under stress and still return to its original shape without permanent deformation. It may be used in a wide range of applications thanks to this unique quality [9–12]. Several types of rubber have been investigated in the literature, including natural rubber (NR), ethylene-propylene-diene monomer (EPDM), polypropylene (PP), styrene-butadiene rubber (SBR), polybutadiene rubber (BR), isobutylene isoprene rubber (IIR), and styrene-butadiene-styrene rubber (SBSR). According to numerous sources, recovered high crosslink density of rubber are responsible for the material's increased tensile strength and modulus. The increase in adhesion between virgin rubber and recycled rubber increases elongation at break of composites [12–19]. When recycled EPDM rubber is added to virgin rubber, EPDM increases the crosslinking density of the elastomer [13]. In rubber mixtures with natural rubber and SBR, tensile strength, tear strength, hardness, and modulus of elasticity generally increase with the increasing amount of SBR particles, while the elongation at break is lower than the unfilled natural rubber [9–15]. Another study by Debapriya and Debabish [11] showed that adding more recycled rubber to SBR increases tensile strength, modulus, elongation at break, and hardness. According to Xiaoou [16], adding filler to recycled rubber increases tensile strength, while decreasing elongation at break when the amount of filler is increased. This shows that the strength and rigidity are significantly improved. Khaled [15] reported that using recycled rubber as an alternative to virgin rubber may cause a reduction in elasticity. This may be due to the fact that the addition of recycled rubber shortens the length of rubber polymer chains. According to Nesrawy [17], mechanical properties of NR/SBR blends improve with an increase in the amount of recycled rubber. Hardness, tensile strength, tear resistance, and modulus all increase, but elongation at

break decreases [15–18]. The matrix affects the damping properties of composites that use energy depending on the mechanism of stress transfer between matrix and reinforcement. In a study on dynamical mechanical analysis, damping factor, storage moduli, and loss moduli of filled recycled rubber composites are reported [17]. A greater filler content reduces the damping factor while increasing the storage and loss moduli. According to Debapriya's study on viscoelastic behavior, the storage and loss moduli increases steadily as the amount of recycled rubber increased. Their findings suggested that recycled rubber improves the viscoelastic properties of the rubber compositions. When recycled EPDM is added to natural rubber, Nabil et al. [18] observed an increase in the storage modulus of the natural rubber vulcanizates due to the high crosslink density in recovered EPDM. Sukanya S. et al. [19] have investigated the characteristics of composite with recycled rubber (RR) and waste polyethylene (WPE). With an increase in the RR amount in the composite, it is seen that the tensile strength decreases whereas the elongation at break increases. The elongation at break increases from 101% for WPE to 789% for the WR70 blend. The flexural strength and flexural modulus of the WPE:RR blends decrease with an increase in RR content.

Strength and stiffness of rubber are essential to its functionality; these mechanical properties cannot be enhanced purely chemically. To enhance its low strength and modulus, it should be reinforced using a filler that is stronger and stiffer [10–12,20–22]. To enhance physical properties, develop design flexibility, reduce the cost of cured rubber, develop mechanical properties, such as fracture toughness and resistance to impact, fillers are used as reinforcement materials in the production of rubber composites [20–25]. Different properties are necessary for an ideal reinforcing depending on the type of filler. A variety of micro- and nanoscale particles, such as glass bubble (GB), glass fiber (GF), aluminum powder (Al), alumina fiber (Al_2O_S) (AF), nanosilica (SiO_2), iron oxide (Fe_3O_4), graphene nanoplatelets (GnPs), boron nitride (BN), and carbon nano tubes (CNT) are used as reinforcement of composites. The majority of the studies on recycled rubber composites show that recycled rubber reinforced with fillers lead to the development of physical and mechanical properties of the structures and also provide low-cost and lightweight composites for several application areas.

2. Mechanical Behavior of Reinforced Recycled Rubber Composites

The data for basic material parameters of recycled rubber composites are critical for a successful engineering development process. In addition, different characterization methods are used to examine the physical and mechanical properties of these composites.

GBs, also called hollow glass microspheres (HGMs), are an alternative to commonly used inorganic fillers, such as silica, calcium carbonate, and talc, for many uses of reinforced rubber composites [25,26]. They have high strength to density ratio for use in demanding polymer processing operations for various rubber parts and applications. A perfectly spherical shape with an aspect ratio of one makes glass bubbles efficient volume fillers and they, when used with other reinforcing fillers in an optimized formulation, can provide excellent energy absorption, weight reduction, and dimensional stability characteristics [24–26]. Since GBs reinforced rubber composites have high damping characteristic, they are used in automotive industry applications and in suspension systems and bumpers of the automobiles due to its energy absorption capacity. They are expected to have promising results. In the literature, there is a limited number of comprehensive studies on recycled rubber composites reinforced with glass bubbles and short glass fibers. However, the following studies provide the basic idea on the mechanical behavior of these reinforcements when used with recycled scrap rubber as well as some other matrix polymers.

Mechanical properties of HGMs epoxy composites are investigated by Bhatia et al. [25]. The mechanical properties of epoxy matrix reinforced with HGMs of 220 kg/m^3 in 60 and 30 vol% are studied. With increasing volume fractions of the reinforcements, the compressive strength of HGMs filled epoxy composites decreases according to Figure 1a. Furthermore, HGMs with higher density provide a higher compressive strength. The change in compres-

sive strength-modulus with respect to the density of HGM filled composites is presented in Figure 1b. This graph shows that compressive strength of composites increases if the density of reinforcements increases. Changing the wall thickness and volume fraction of HGMs, on the other hand, has a negligible effect on compressive strength. The maximum compressive strength of HGM polymer composites with HGM is also researched in that study and the maximum compressive strength has been recorded for 10% or less content of HGM. In some composites, a higher HGM content can provide higher values of modulus of elasticity. The stress-strain curve obtained by tensile tests is shown in Figure 1c representing that the composites show brittle failure. It shows that these composites are limited to applications with compressive loading due to the reduced tensile properties. However, thick-walled HGMs increase the tensile modulus of composites as can be seen in Figure 1d. The tensile strength of HGM composites can be improved by adding glass fibers, carbon fibers, carbon nanotubes, and other fillers [27–30]. The graphs of flexural strength and modulus-density for thin and thick-walled HGMs are shown in Figure 1e,f. It is observed that as the volume fraction of thin-walled HGMs increases, the flexural modulus increases slightly. Incorporating a higher percentage of thick-walled HGMs, on the other hand, substantially decreases the flexural modulus as seen in Figure 1f.

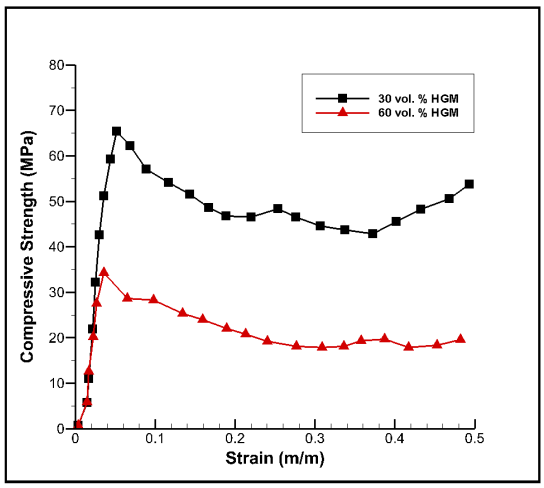

(**a**)

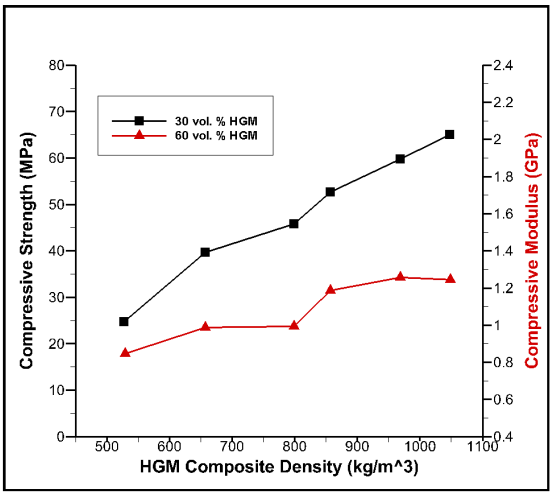

(**b**)

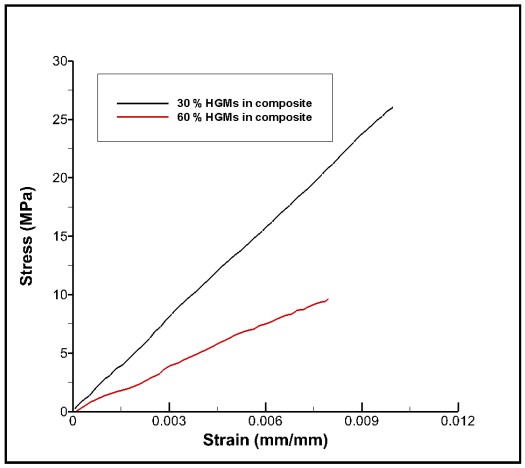

(**c**)

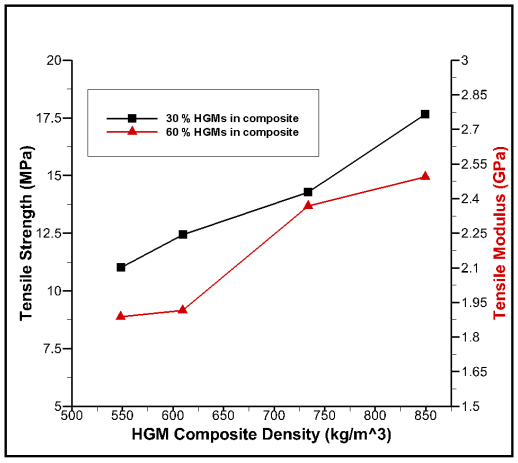

(**d**)

Figure 1. *Cont.*

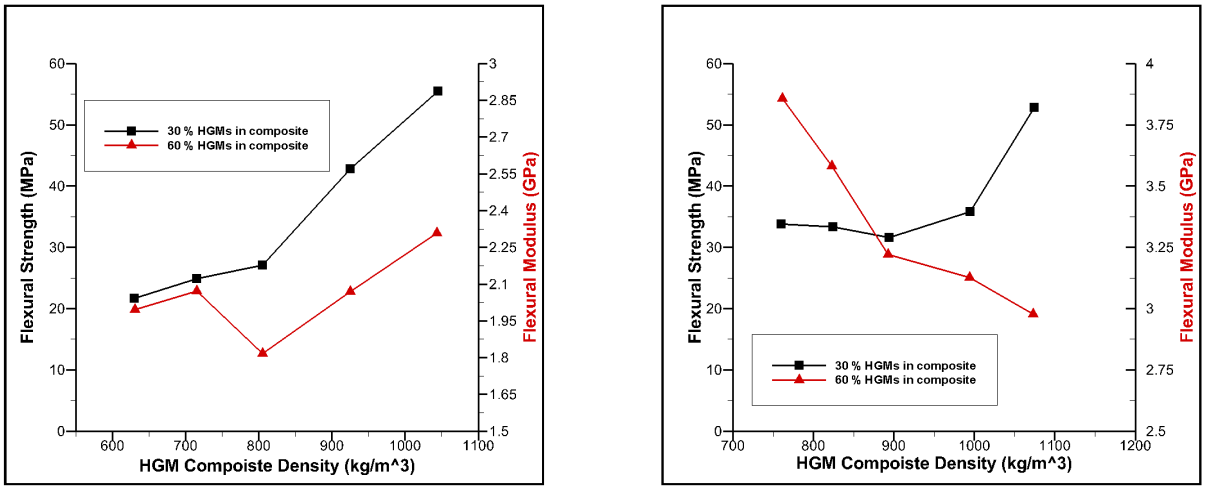

Figure 1. (**a**) Compressive stress-strain curve of epoxy matrix with HGMs. (**b**) Variation in compressive strength and modulus regarding the HGM composite density. (**c**) Tensile stress-strain curves of HGM composites. (**d**) Variation in tensile strength and modulus regarding the HGM composite density. (**e**) Variation in flexural strength and modulus with HGMs of 150 kg/m^3 density. (**f**) Variation in flexural strength and modulus with HGMs of 460 kg/m^3 density [25].

A high-performance polymer is prepared with GB content of up to 40 and 60 wt% to determine density and mechanical properties, such as tensile strength and flexural stress [25–34]. A density reduction of 24% is achieved for composites with 40 wt. % of glass bubbles. In tensile and flexural tests, hollow glass microspheres are observed to increase the modulus and tensile values by the increasing content of fillers as seen in Figure 2a,b, respectively.

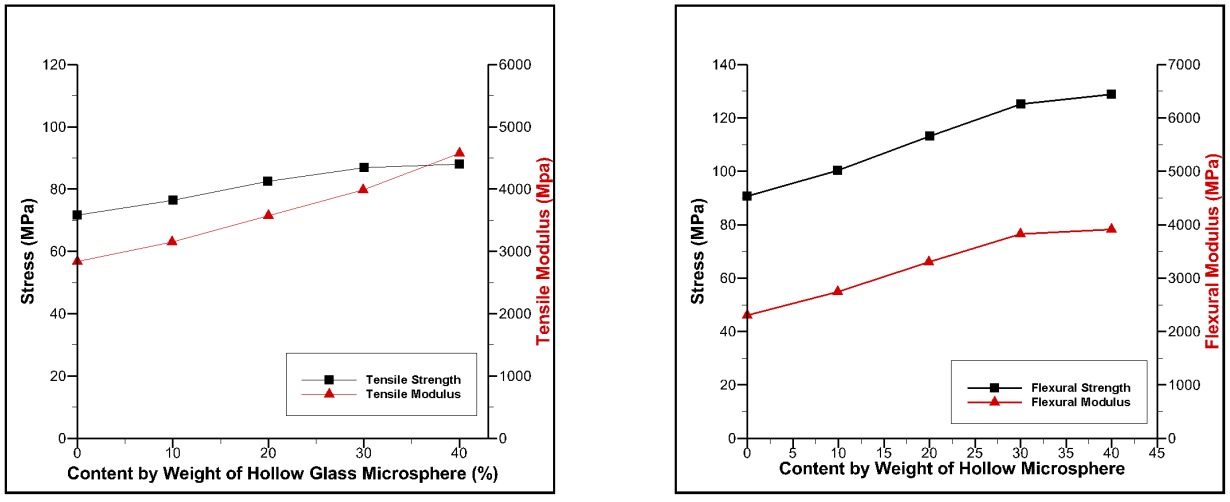

Figure 2. (**a**) Tensile test results. (**b**) Flexural test results [28].

The mechanical properties of the composites based on recycled polypropylene (rPP), SBS with 30 wt. % SIS and GBs with diameter varying between 16–65 µm are analyzed by Râpa et al. [28]. Table 1 shows the compositions for rPP composites reinforced with GBs used in this study. The effect of the content of glass bubbles on the mechanical properties of rPP composites, such as density, tensile strength, elongation at break, are presented in Table 2. Therefore, the density of recycled polypropylene with SBS is decreased from 1.018 g/cm^3 to 1.0007 and 0.9826 g/cm^3 by adding 5% and 20% GBs, respectively. Without

the elastomer, GBs are expected to increase the density of rPP composites while decreasing elongation and tensile strength. In comparison to neat rPP, the tensile strength of rPP/SBS composite decreased by 18.5% at 10% elastomer content, and by 17% in the case of rPP/SIS composite [28]. The tensile strength of virgin PP/elastomer blends and PP waste/elastomer blends has also been stated to be decreased due to the inability of elastomer and polypropylene to form a homogeneous phase, as well as the low strength amorphous rubbery matrix [26–32,35–64]. The tensile property of rPP/SIS and rPP/SBS composites is increased when glass bubbles are introduced into the composites. In contrast to unmodified post-consumer rPP, elongation at break increased significantly due to the elastomer effect, which acted as a plasticizer and allowed for better material stretching [28,59,63].

Table 1. Compositions for recycled polypropylene (rPP) composites [28,58].

Composition	rPP (wt%)	GB (vol%)
rPP	100	-
rPP/SBS	90	-
rPP/SBS/GB5	89.1	5
rPP/SBS/GB20	86.7	20
rPP/SIS	90	-
rPP/SIS/GB5	89.1	5
rPP/SIS/GB20	86.7	20
rPP/GB8	92	14.55

Table 2. Mechanical test results for recycled polypropylene reinforced with glass bubbles [28,58].

Composition	Density (at 23 °C) (g/cm^3)	Tensile Strength at Break (MPa)	Elongation at Break (%)
rPP	1.0158	26.98	30.30
rPP/SBS	1.0180	21.99	72.22
rPP/SBS/GB5	1.0007	21.36	46.36
rPP/SBS/GB20	0.9826	20.45	40.30
rPP/SIS	1.0173	22.39	55.20
rPP/SIS/GB5	1.0001	23.51	38.78
rPP/SIS/GB20	0.9494	24.22	26.69
rPP/GB8	0.853	29.8	3.67

GFs have high strength with low density. The tensile modulus and yield stress of the recycled rubber composites are enhanced with the increasing content of GFs [29–33]. They provide toughness improvement in rubber composites which increase the plastic zone in the structure and this leads the composites to dissipate additional fracture energy. Yu et al. have investigated the effects of increasing the content of glass fibers and polypropylene fibers in epoxy polymer to reduce cost and improve mechanical performance. This has shown that short fibers enhance the flexural performance, while the crumb rubber improves the flexibility of polymer composites [30–32]. In Table 3, the variation of the tensile modulus and tensile strength of the recycled HDPE composite with PP including 35 wt% of GFs (PP-GF (35)) is presented [30,31]. As seen in this table, the mechanical performance of recycled HDPE is improved.

Table 3. Mechanical properties of recycled HDPE composite with PP-GF (35) [29–31].

PP-GF (35) in HDPE (wt%)	Tensile Modulus (GPa)	Tensile Strength (MPa)
0	1	14
10	1.1	16
20	1.5	20
30	2	25
40	2.7	28
50	3.3	31

Furthermore, short glass fibers are applied as reinforcement in recycled high-density polyethylene and ground tire rubber (GTR) composites [33–35]. In that study, the HDPE composite is mixed with different compositions of PP-GF (30). Figure 3a,b shows the variations of the tensile properties with the weight percentage of PP-GF (30). The tensile modulus and yield stress are enhanced with the PP-GF (30) content for both polyethylene composites.

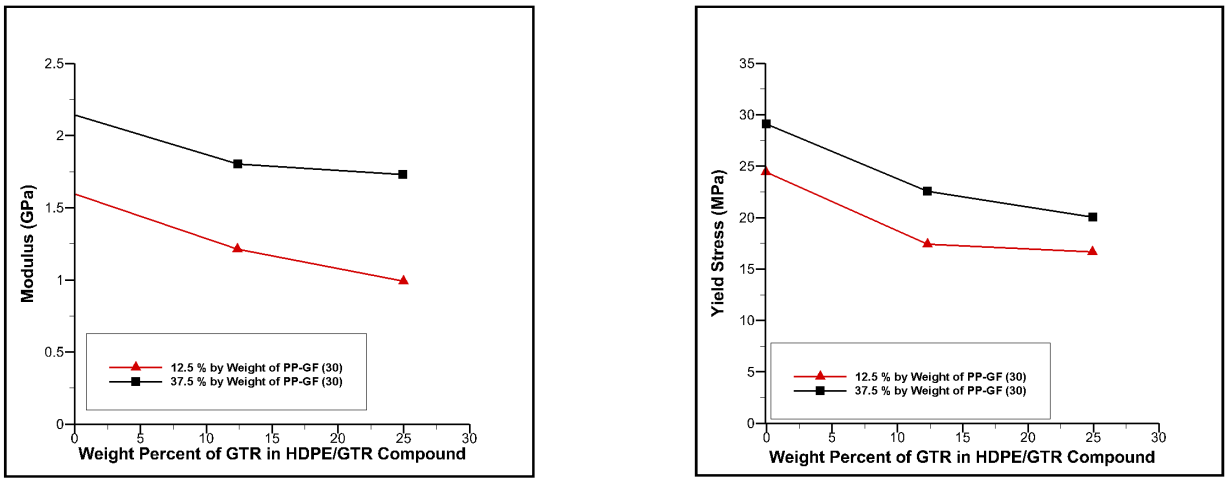

(**a**) (**b**)

Figure 3. (**a**) Variation of the tensile modulus with the GTR content for the HDPE/GTR/PP-GF (30) composites. (**b**) Variation of the yield stress with the GTR content for the HDPE/GTR/PP-GF (30) composites [30,31].

Then, aluminum is an inexpensive material and increases the surface hardness when used as reinforcement in rubber composites. The mechanical behavior of recycled rubber composites filled with Al is investigated by Allouch et al. [32]. In Table 4, the composition in parts per hundred resin (phr) of each composite prepared in the study is presented. Moreover, the tensile strength and the elongation at break of the composites are presented in this table. As aluminum powder content is increased, tensile strength of the composite is improved. The elongation at break, on the other hand, shows that composites reinforced with Al have worse properties than virgin materials. This is the reason that metallic reinforcements reduce the elasticity of rubber matrix chains, resulting in breaking at lower elongation and also increase in hardness [31]. Therefore, by adding Al, the stiffness of the composite increases.

Table 4. Weight percentage of the recycled rubber reinforced polymer composites filled with aluminum powder [31].

Compound	NR (phr)	Recycled Rubber (phr)	Al Powder (phr)	Tensile Strength (MPa)	Elongation at Break (%)
C1-00	20	80	0	1.95	103
C2-10	20	80	10	1.63	75
C3-20	20	80	20	1.87	75
C4-30	20	80	30	1.89	65
C5-40	20	80	40	2.24	66

BN has high hardness and thermal stability. It increases the crosslinking density and decreases the polymer chain mobility. Furthermore, nanosilica are found to be efficient in improving the chemical characteristics of the matrix [33–35]. SiO_2 reinforced recycled rubber composites are aimed to be used in wing spars. Devulcanized fine-scrap-rubber powders (EPDM) are reinforced with GBs, Al, and BN, and the chemical compositions of these fillers are provided in Table 5 [34,35]. Mechanical properties shown in Table 6 show that the addition of GBs, BN, and Al improve the mechanical properties of the composite compared with those of the matrix. The addition of GBs to devulcanized scrap rubber powders with BN and Al result in an increase in the strain at break. Moreover, in research, it is observed that the density is decreased by the addition of glass bubbles to the composite. For example, the density of the composite ENRF I is 1.823 g/cm^3, whereas it is 1.81 g/cm^3 for ENRF II.

Due to high magnetic and structural properties of Fe_3O_4, composites are manufactured for electronical applications in aeronautic industry and in antenna systems of the aircrafts. Recycled and devulcanized SBR composites reinforced with Fe_3O_4 are designed by Irez, Bayraktar, and Miskioglu [33,35]. Four different compositions shown in Table 5 are prepared. The size of Fe_3O_4 particles are 45–70 nm and Al particles are smaller than 23 nm. The addition of Fe_3O_4 improves the flexural strength of the composite, as shown in Table 6. Furthermore, the high modulus of iron oxide improves the modulus of the composites, even though a decrease is observed at high reinforcement material. The main effect of iron oxide is observed on strain values. The deformation capacity of composites is significantly reduced as the iron oxide rate is increased. Moreover, an improvement is observed in the flexural strength of composites with the increase in a certain amount of Fe_3O_4. After a point, addition of iron oxide results in the decrease of flexural strength [33–35]. Generally, nano-fillers are found to be efficient in improving the mechanical and chemical characteristics of the matrix [34].

Table 5. Composition of the epoxy-rubber based composites reinforced with GBs, aluminum, boron, and Fe_3O_4 [34,35].

Composite	Reinforcements (wt%)					
	BN	Al	GB	Fe_3O_4	Ni	Silica
ENRF I	5	5	-	-	-	-
ENRF II	5	5	5	-	-	-
ENRF III	10	5	5	-	-	-
EBAL	5	10	5	-	-	-
ENRF IV	-	10	-	10	5	5
ENRF V	-	10	-	20	5	5
ENRF VI	-	10	-	30	5	5

Table 6. Mechanical properties of the epoxy-rubber based composites reinforced with GBs, boron, and Fe_3O_4 [34,35].

Composition	Ultimate Flexural Stress (MPa)	Flexural Modulus (MPa)	Strain at Break (ε %)
Matrix	42.13	7.88	1.44
ENRF I	47.23	9.69	2.36
ENRF II	50.04	9.96	2.47
ENRF III	50.39	11.75	2.30
EBAL	46.61	10.51	1.96
Matrix	42.13	7.88	0.66
ENRF IV	44.83	7.49	0.72
ENRF V	49.31	10.26	0.51
ENRF VI	31.85	9.34	0.39

AFs generally improve fracture toughness [37,38] and have high compressive strength and shear properties [38]. They also have good thermal conductivity, high adsorption capacity, thermal stability, and electrical insulation [36,37]. The recycled rubber composites reinforced with AFs can be used in electronic packaging/underfill for circuit cards, dental restoratives, and automobile parts through its mentioned properties [37–44]. Then, GnPs is an alternative nano-scale material with high elasticity modulus and mechanical strength [43–45]. It has a two-dimensional honeycomb structure and high surface area, thus a low content of these nanoparticles may enhance the material properties [45–47]. Its outstanding properties can be given as specific elasticity modulus and mechanical strength, thermal conductivity, and high electrical conductivity [47–52]. GnP reinforced composites are used in a wide range of applications, such as electrochemical applications, lithium-ion batteries, sensors, solar cells, water purification, and super capacitors [51,52]. High electrical conductivity of GnPs can also reduce the risk of damage to aircrafts from lightning strikes [52,53]. GnP reinforced composites have major improvements in strain and strength. While increasing the GnP content reduces the strain improvement, GnP modification of the composites improves the plastic deformability. In addition, increasing GnP content increases flexural strength proportional to GnP content. Irez [51–54] has studied recycled rubber composites reinforced with AFs and GnPs. The compositions are provided in Tables 7–9. In that study, flexural tests are conducted with EPDM recycled rubber modified epoxy-based composites (LR) and results are presented in Figure 4a, where the numbers in LR10, LR20, and LR30 show the weight percentage (wt%) of rubber content. According to that figure, rubber modified composites, when compared to neat epoxy, fail due to the brittle behavior of the composites. In addition, as the EPDM rubber content increases, the strain at break decreases. Neat epoxy, on the other hand, remains in the plastic region before the fracture. As a result of this figure, it can be deduced that recycled rubbers minimize the deformation capability and EPDM rubbers decrease the strength of the composite [33–35].

Table 7. Characterization of recycled rubber composites reinforced with AFs and GnPs [51–54].

Group Name	Composition
LR	Epoxy + RR
LAL	Epoxy + AF
LG	Epoxy + GnPs
LRAL	Epoxy + RR + AF
LRG	Epoxy + RR + GnPs

Table 8. Composition of the alumina fiber reinforced composites [56].

LRAL Composites	AF Content (wt%)			
Rubber Content	**0%**	**5%**	**7.5%**	**10%**
0%	Neat Epoxy	LAL5	LAL7.5	LAL10
10%	LR10	LR1AL5	LR1AL7.5	LR1AL10
20%	LR20	LR2AL5	LR2AL7.5	LR2AL10
30%	LR30	LR3AL5	LR3AL7.5	LR3AL10

Table 9. Composition of the GnP reinforced composites [53].

LRG Composites	GnP Content (wt%)			
Rubber Content	**0%**	**0.5%**	**1.0%**	**1.5%**
0%	Neat Epoxy	LG0.5	LG1	LG1.5
10%	LR10	LR1G0.5	LR1G1	LR1G1.5
20%	LR20	LR2G0.5	LR2G1	LR2G1.5
30%	LR30	LR3G0.5	LR3G1	LR3G1.5

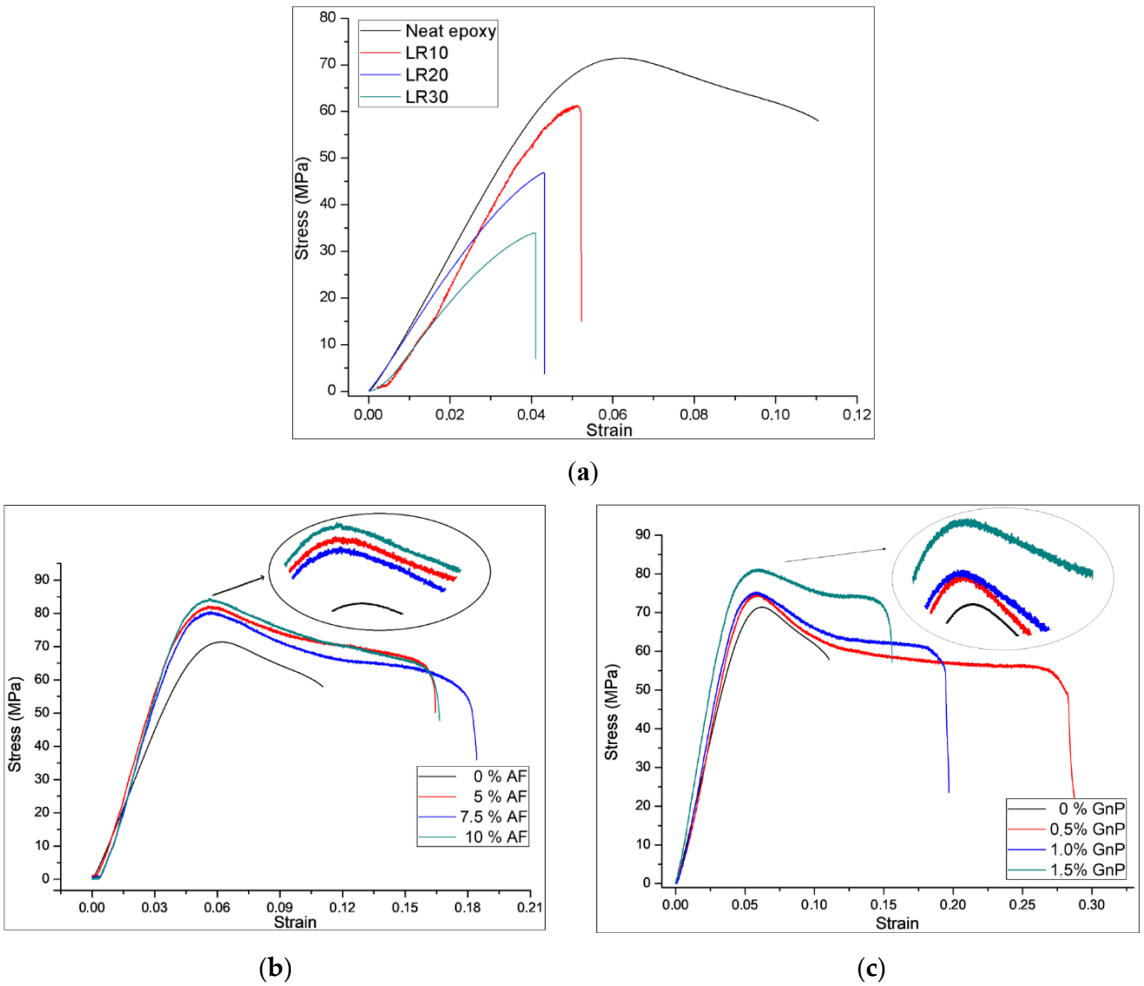

Figure 4. Comparison of stress-strain curves of (**a**) recycled EPDM rubber composites (LR). (**b**) AF reinforced epoxy-based composites (LAL). (**c**) GnP reinforced epoxy-based composites (LG) [54].

The incompatibility of the rubber particles with the epoxy resin matrix is the main reason for the lack of improvement in recycled rubber modification. Owing to a lack of free links that can establish bonds with the resin and particles, rubber particles do not interlock well with the matrix. As shown in Figure 4b, AFs significantly improve the elongation characteristics under quasi-static loading and these composites remained in the plastic field for a long amount of time. As a result, AFs develop the ability to absorb mechanical energy when subjected to static loading. One of the reasons for high strength values is the presence of hard microparticles retarding the propagation of microcracks in the microstructure [51–54]. Figure 4c illustrates that GnP reinforced epoxy-based composites have major improvements in strain and strength. While increasing the GnP content reduces the strain improvement, GnP modification of the composites improves the plastic deformability. In addition, increasing the GnP content increases the flexural strength proportional to GnP content. The agglomeration of GnPs may be the reason for the decreased strain efficiency of these composites.

The stress-strain curves for all LRAL composites are shown in Figure 5, showing that as the amount of rubber in the composites increases, the strength of the composites decreases. In addition, as the rubber content increases, the slope of the curve before maximum stress is reached decreases. This indicates that the modulus of elasticity decreases. Strain at break, on the other hand, shows some variation depending on the rubber content in the composite. The flexural modulus shows the main improvement due to the rigid characteristic of AFs. Results of the 3PB bending tests of the recycled rubber composites reinforced with GnPs are presented in Figure 6. In this figure, as with binary composites, the strength level of the composites decreases as the rubber content increases. In addition, the stress responses for the LG and LR1G composites are progressing smoothly. The layered structure of the GnPs causes a delay between the load increase and the strain as the cracks propagate. However, for the LR2G and LR3G composites, the increase in rubber content shades this behavior for the composites [53,54]. In general, flexural modulus, strength, and strain at break are improved by the increasing amount of GnPs.

CNTs have high thermal and electrical conductivity. They are highly flexible and have very high tensile strength. In aeronautical engineering applications, CNT reinforced rubber composites are utilized [53,54]. The composites reinforced with AF and GnPs with CNTs have shown enhancements in the mechanical properties, and more significantly, flexural stress and fracture toughness [53,54].

Zaghloul et al. have studied mechanical behaviors of polypropylene composites adding two types of carbon fillers to polypropylene-carbon nanotubes and synthetic graphite. It is observed that they lead to a remarkable increase in the flexural and tensile modulus of the composites [55,56]. They have also observed mechanical properties of linear low-density polyethylene fire-retarded with melamine polyphosphate (MPP) and it is observed that the Young's modulus, flexural modulus, the tensile fracture strength, and tensile yield strength increase with the increasing MPP content [57,58].

The determination of physical and mechanical properties of these composites is realized using various characterization methods and they offer an effective mechanical performance based on strength, elasticity modulus, and strain values.

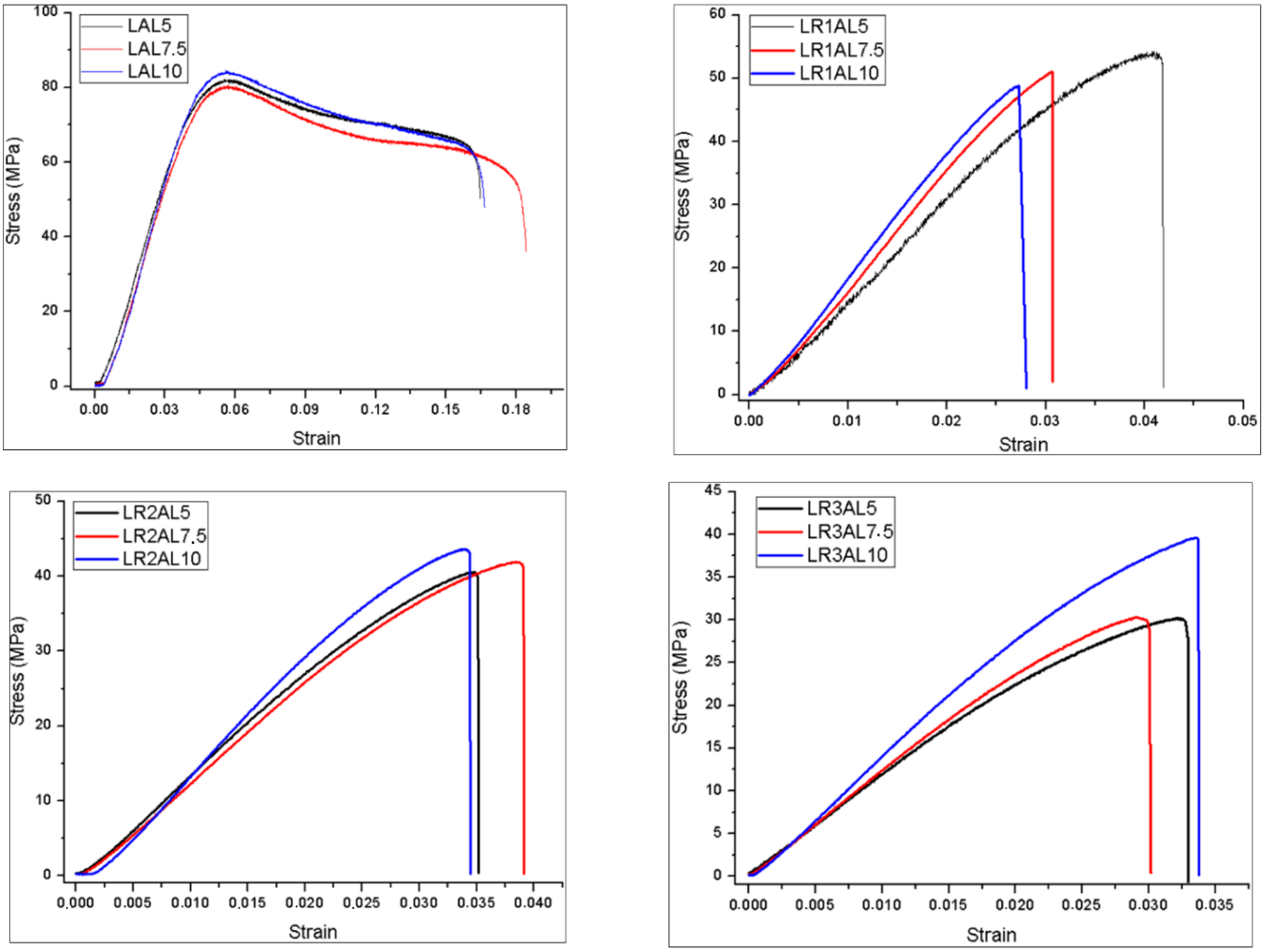

Figure 5. Stress-strain curves of the recycled rubber composites reinforced with AFs (LRAL) [53].

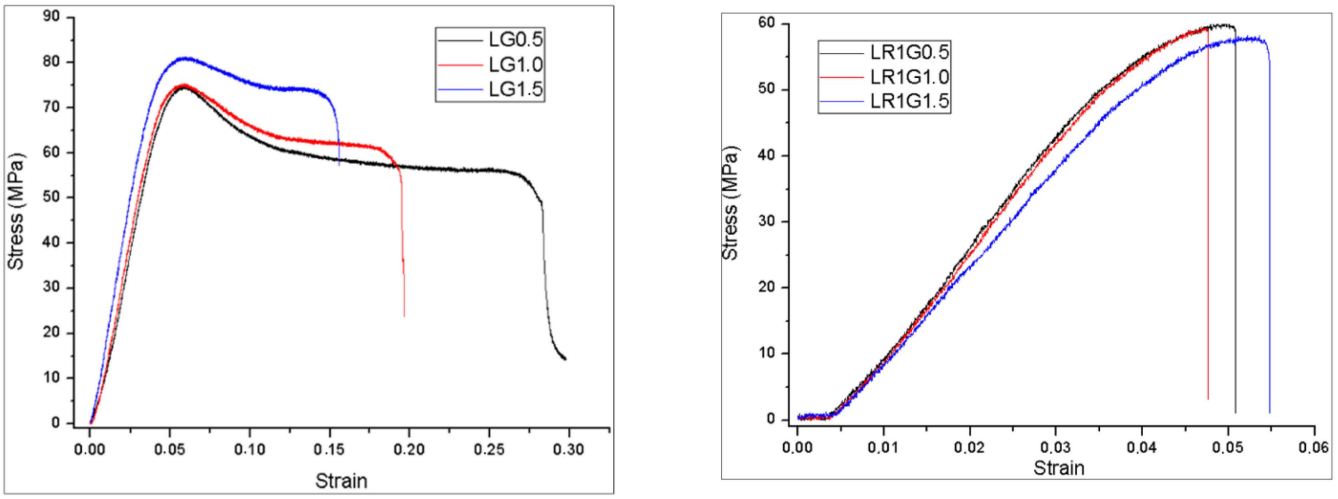

Figure 6. *Cont.*

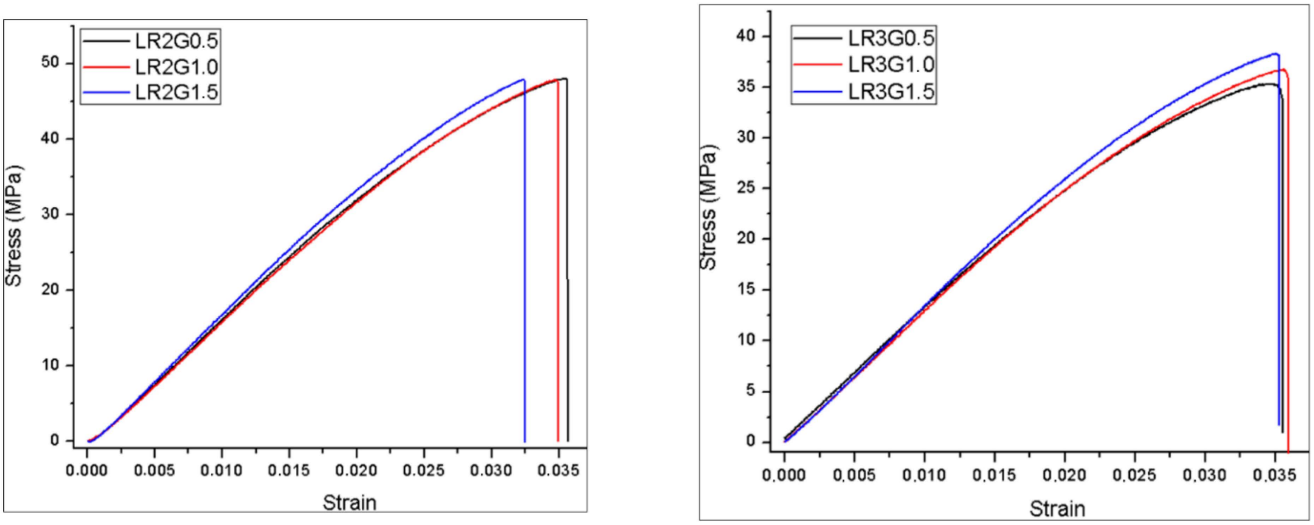

Figure 6. Stress-strain curves of the recycled rubber composites reinforced with GnPs (LRG) [53,54].

3. Microstructure and Fracture Toughness Determination

Microstructure and surface damage evaluations are commonly made by means of optical microscope (OM) and scanning electron microscopy (SEM). SEM observation is realized on fracture surface of the tested specimens with electron microscope. Creating an ideal interface for each composition is needed to observe good adhesion of both reinforcements in the rubber-based matrix. Cavitation and void formation in the rubber matrix with matrix expansion and locally, debonding of nano particles with consequent void growth can be identified in the structure as the improved toughening mechanisms. Crack propagation, crack growth, and crack extension are analyzed by fracture mechanics. Cracks and defects can take place in the recycled rubber composites during their manufacturing or some discontinuities may occur inside the microstructure causing fracture in the materials. As a result, considering the fact that the yield strength is not always the most effective way to design the composites, this is the reason that cracks can cause fractures in the material at lower loads. Therefore, fracture mechanics is regarded as the best option to solve these issues [64,65]. Numerical measurement of the resistance to crack propagation under loading is defined as fracture toughness and a material with higher fracture toughness would be less likely to propagate cracks. According to Donald [64], composites have a higher fracture resistance than many other types of materials. Three critical variables must be considered during the design and material selection process of the composites, such as fracture toughness, also known as the critical stress intensity factor, K_{Ic}; the stress, σ that the material must resist; and the crack size, a. Following that, K_{Ic} should be large enough to prevent crack propagation and the dimension should then be selected in order that the maximum stress is not exceeded [65–67]. Fracture toughness is calculated using a variety of methods based on the fracture behavior of the material. When the fracture characteristics are well established, the hypotheses for determining fracture behavior produce more accurate results. Furthermore, some parameters influencing material behavior, such as loading rate, may change the fracture toughness calculation. The fundamental approaches can be described as linear elastic fracture mechanics (LEFM) and elastic-plastic fracture mechanics (EPFM). Mechanical tests are performed after the composites are manufactured. In the literature consisting of the research discussed in that study, the composites generally remain elastic until maximum stress is reached during 3PB tests. Then, the composites experience a sudden rupture indicating that rubber modified composites have brittle characteristics. General microstructure in the transversal direction of the ENRF compositions are shown in Figure 7a [35]. Microstructural observation shows a homogenous distribution of the reinforcements in the microstructure and the adhesion of the rubber to the epoxy matrix is very successfully carried out. Some of the local agglomerations of rubber particles

are observed in the microstructure. This indicates that homogenous distributions of the reinforcements need more mixture process [35].

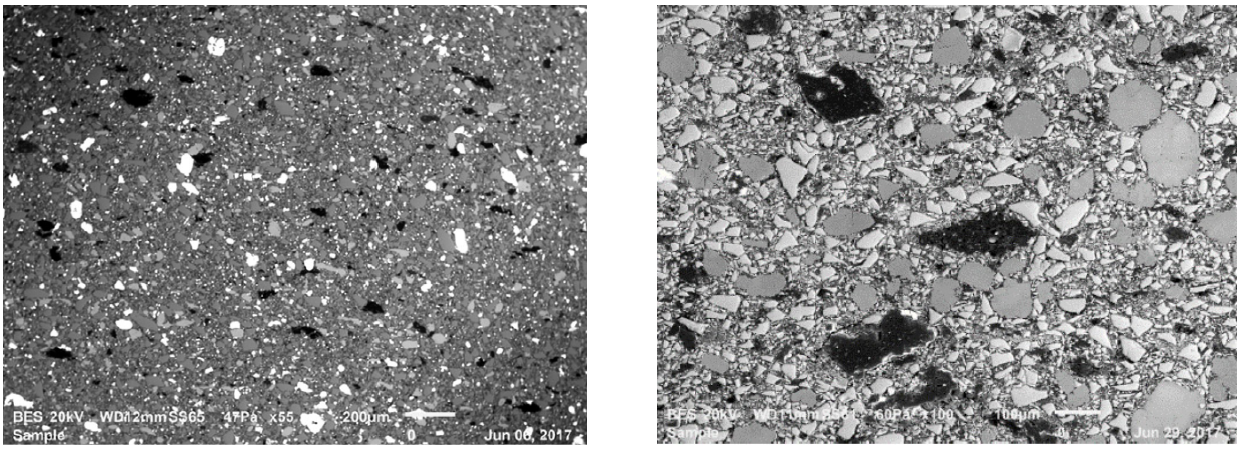

(**a**) (**b**)

Figure 7. General microstructure of the composite. (**a**) ENRF [35]; (**b**) EBAL [34].

General microstructures are presented in Figure 7b for the composite EBAL [34]. The composition shows a homogenous distribution of the reinforcements in the structure. There is a general homogeneity observed in the distribution of the particles in the microstructure although some particles are locally agglomerated. Moreover, there is good cohesion between the matrix and the inclusions at the interface [34].

Figure 8 shows scanning electron microscopy (SEM) observation of PA6 and hollow glass bubble composites. The HGMs are optimally bonded to polymer matrix, which increase the mechanical performance of the composites [28]. The SEM analysis is also performed on the compatibilized rPP, with SBS or SIS block copolymers and composites that contain 5% and 20% of GBs, confirming the presence of impurities. The SBS elastomer is observed as small and dispersed domains in the continuous polymeric phase. The good dispersion of elastomer is observed in the case of SIS. The GBs are evidenced as an encapsulated filler inside the melted samples (Figure 9a–c).

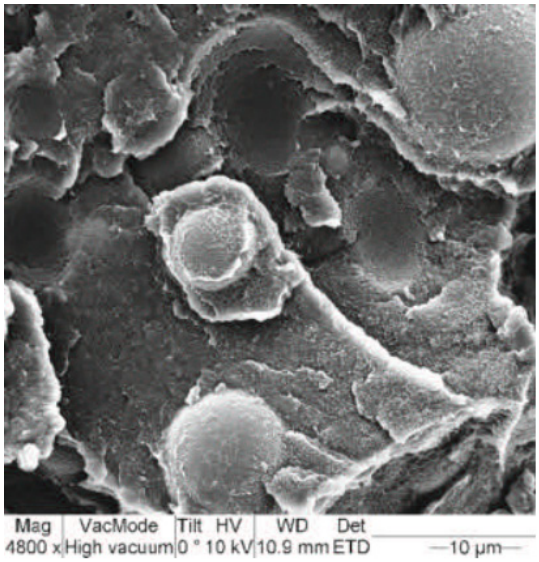

Figure 8. SEM observation for PA6 and hollow glass bubble composites [28].

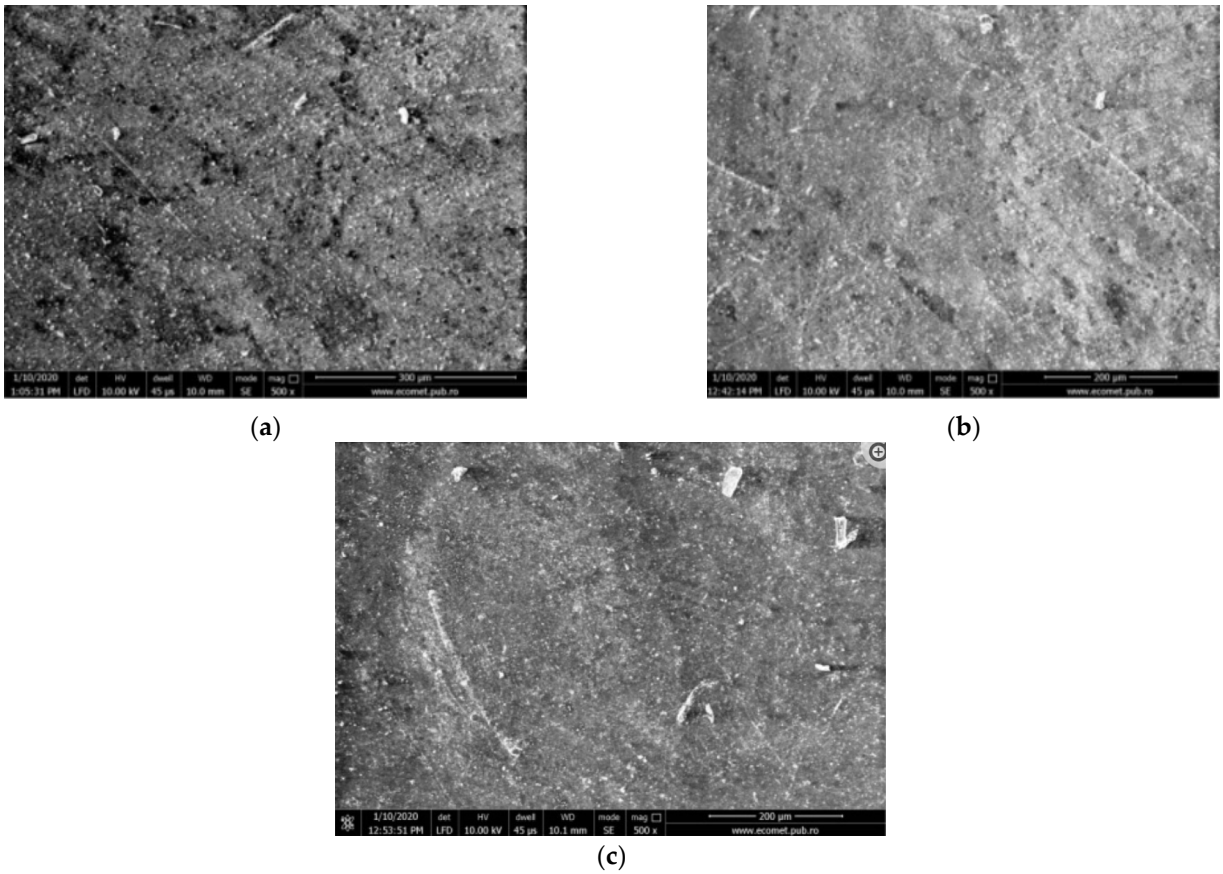

Figure 9. Scanning electron microscope (SEM) images for (**a**) rPP/SBS/GB5 (scale bar 300 μm); (**b**) rPP/SIS/GB5 (scale bar 200 μm); (**c**) rPP/SIS/GB20 (scale bar 200 μm) [28].

Figure 10a shows an SEM image of fracture surface of HDPE containing 37.5 wt% PP–GF. The glass fibers are uniformly distributed within the matrix, and the fibers are mostly oriented along the flow direction during the injection molding. The uniform dispersion of the glass fiber shows good adhesion to the surrounding matrix, and this denotes the effectiveness of the PP–GF system in reinforcing the HDPE-based composites. The SEM micrograph also indicates that the fiber length ranged from 200 to 500 μm in the final product. Figure 10b illustrates the morphology of a sample containing both glass fiber and GTR, namely, the sample [PE(2)/GTR(25)]/[PP–GF(30)](37.5). The picture shows the poor adhesion of the GTR particle to the matrix. In addition, the presence of GTR in the composite slightly disturbed the orientation of the glass fiber due to the melt flow, and this may have been partly responsible for the reduction of the stiffness of the composites containing GTR particles along the flow direction [30,31].

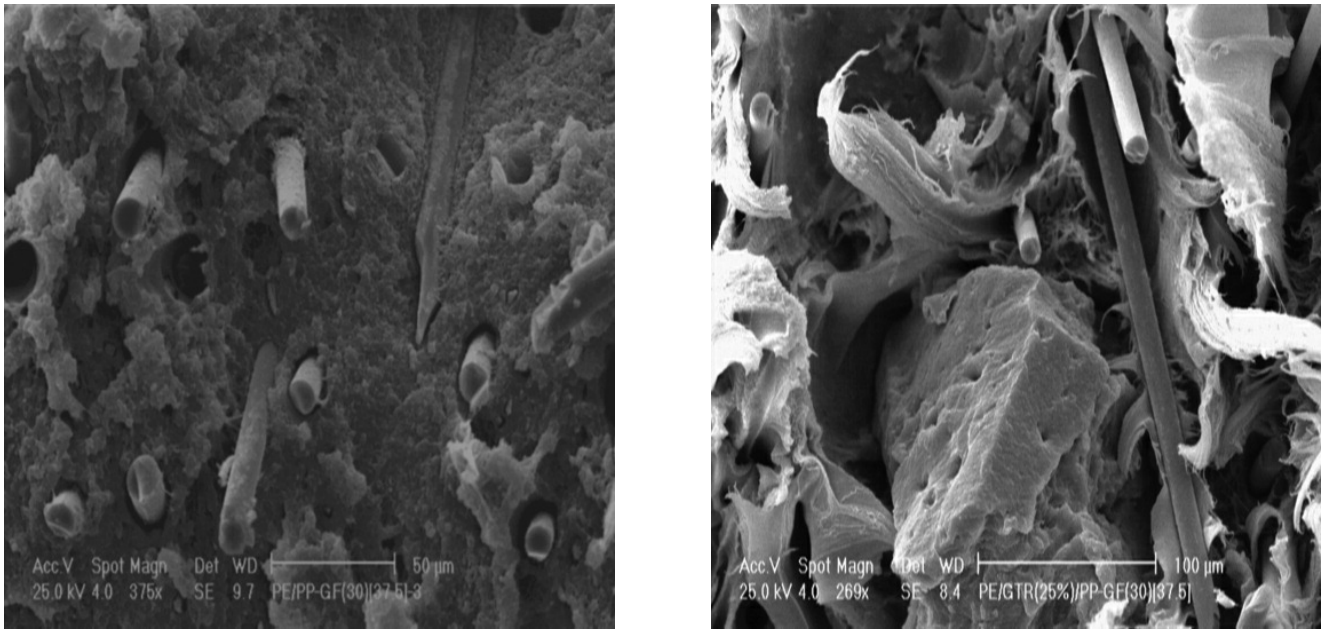

(**a**) (**b**)

Figure 10. (**a**) SEM micrograph of the fracture surface of HDPE filled with 37.5 wt% PP–GF; (**b**) [PE(2)/GTR(25)]/[PP–GF(30)](37.5) [31].

In Figure 11, a sectioned specimen is used to observe the microstructure of the AF reinforced ternary composites by means of SEM and transmitted light microscope (TLM). According to this figure, homogenous distribution of the reinforcing agents is successfully realized. These images are supported with energy dispersive X-ray spectroscopy (EDS) mapping on the sectioned specimens [53].

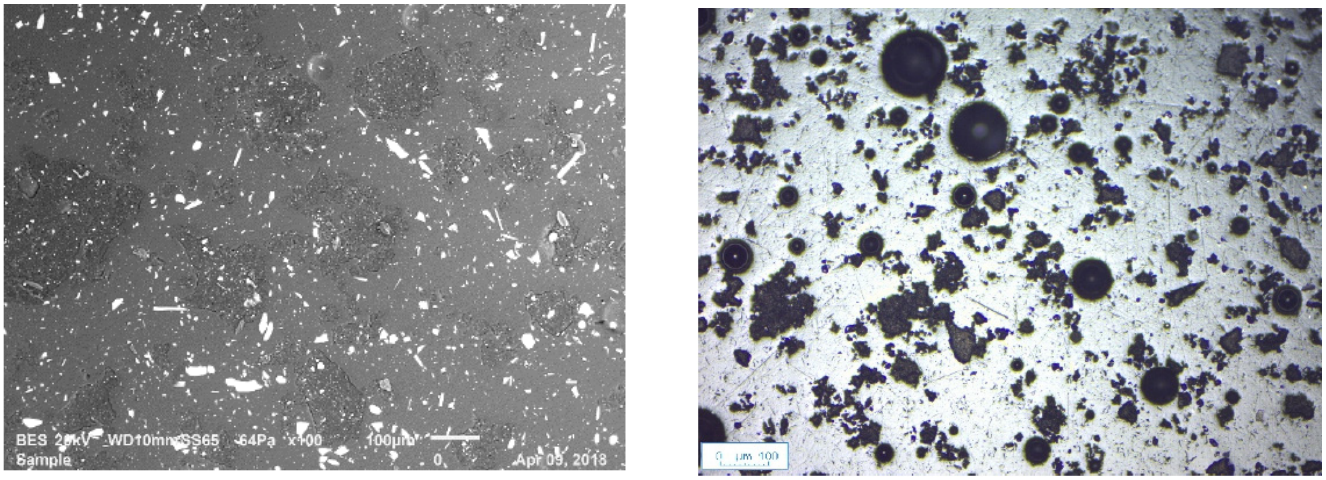

(**a**) (**b**)

Figure 11. Microstructural observation of LR2AL10 by means of (**a**) SEM; (**b**) TLM [53].

Microstructural observation is maintained for LR2G1 and LR20 compositions as shown in Figure 12. These microstructures show homogenous distribution of rubber particles without any remarkable agglomerations. Moreover, the dimensions of the rubber particles show a wide spectrum from 10 to 130 µm. On the other hand, distribution of GnPs requires the microscopical observation at very high magnification [53].

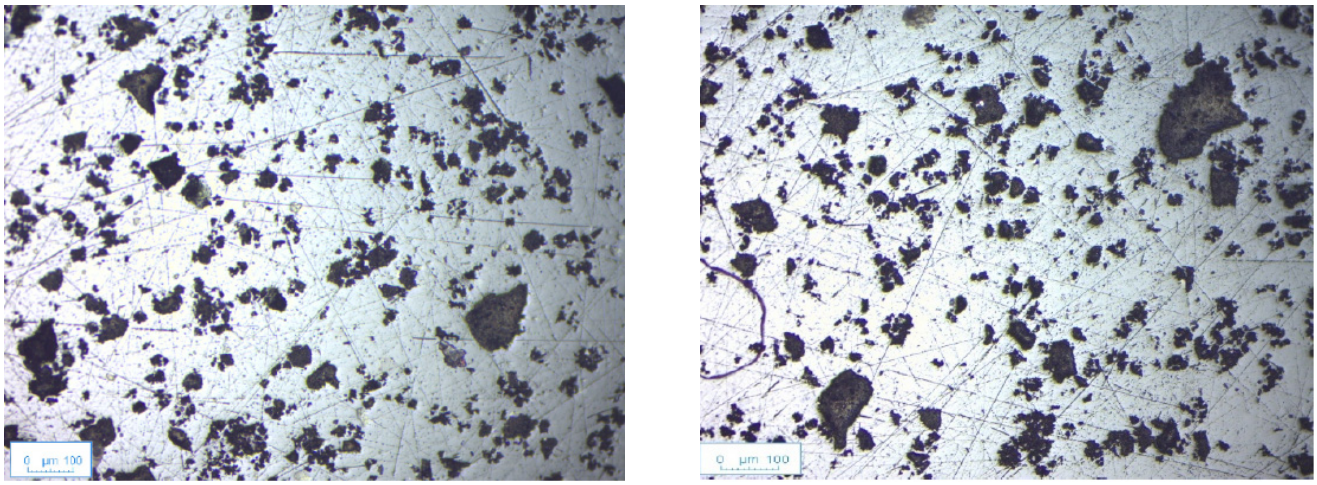

(**a**) (**b**)

Figure 12. Microstructural observation of (**a**) LR2G10; (**b**) LR20 by means of TLM [53].

4. Discussion

The impact of the scrap rubber on the environment can be reduced if it is recycled, and one area to utilize the recycled rubber is in the manufacturing of novel composites. Composites with recycled rubber could potentially have significant advantages over conventional composites considering its desirable and cost-effective dynamic properties. In this study, low-cost devulcanized recycled rubber composites designed with a variety of nano- and microscale reinforcements are compared by means of mechanical and physical properties as well as microstructural analysis. This review covers the aspects of recycled rubber that are recovered from devulcanization.

Studies on recycled rubber composites show that reinforced recycled rubber composites have a great potential on the improvement of physical and mechanical properties providing low-cost and lightweight composites for various application areas, where high toughness and high resistance to impact are desirable. In addition to these studies, dynamic properties of recycled rubber are known to be desirable for many applications and it is important to design a recycled rubber composite that is specifically designed for energy absorption. However, a small amount of work has been performed on GBs in the literature. The reinforcements, such as microsphere glass bubbles, may be new alternative ingredients providing desirable mechanical properties and improving the energy absorption capacity of the composite. Investigation of the effect of those reinforcements for different volume ratios can be studied as a future work.

Mechanical tests on the composites reinforced with AF show that the reinforcement improves the fracture toughness of the composites [53,54]. In those composites, numerical studies indicate that the energy release rate shows some variations along the specimen thickness. By considering the advantageous effects of AF on the novel composites and cost efficiency under favor of recycled rubbers, these composites are promising candidates to manufacture the various components in automotive industry [53–55]. According to scanning electron microscopy, nanoindentation, 3PB test results for recycled and devulcanized rubber composites reinforced with nanomagnetic iron oxide, and nano aluminum powders, there is a combined effect of toughening mechanisms with high strength and ductile, lightweight, and low-cost composites [35]. Mechanical test results show that the reinforcement with graphene nanoplatelets, GnPs, generally increased the modulus of elasticity as well as the fracture toughness of these novel composites. Moreover, it is observed that these composites have the potential to be used to manufacture various components in the automotive and aeronautic industries, as well as smart building materials in civil engineering applications [53–55]. Fracture surfaces of the compositions reinforced with gamma-alumina have shown that there will be strong cohesion between the reinforcements

and matrix if the homogenous distribution of the reinforcement in the matrix can be provided. The rubber-based composites reinforced with microscale particles with a certain ratio have shown improvements in the fracture toughness.

Although their basic mechanical behavior has been extensively studied in the literature, a comprehensive numerical model considering the microstructure of these composites does not exist in the literature. To date, few studies that are carried out on numerical analysis have been mentioned at that point. Continuum structures of polymer nanocomposites are modelled, and their mechanical properties are predicted by finite element method and micromechanics in the literature [68–79]. Halpin–Tsai model, Nielsen's model, Mori–Tanaka model, Eshelby model, modified rule of mixtures and Shear Lag models, equivalent continuum model, and self-consistent model are some of the continuum methods used in polymer nanoparticle composites [70–78]. These micromechanics models provide the prediction of the elastic properties of nanocomposite materials based on the geometry, orientation of the filler, and elastic properties of the filler and matrix. The Halpin–Tsai model is commonly used to predict the effective stiffness for fiber reinforced composites with perfect fiber alignment. Then, Mori–Tanaka is an effective field theory for inhomogeneity in an infinite medium to predict the modulus of nanocomposites. When micromechanical models are applied to nanoparticle composites, some assumptions are considered in order that fillers behave as linearly elastic materials, perfect bonding exists between reinforcements and matrix, the reinforcements are axisymmetric, identical in shape and size, and can be described by their aspect ratio [75–77]. Finite element analysis is used for modelling of polymer nanoparticles with low nanoparticles content [76–79]. It has been obtained that the nanoparticles should be distributed uniformly in the matrix. A modified Halpin–Tsai homogenization model is adapted to the rubber-based composites to estimate the moduli of the composites by Kabakcı, Aslan, and Bayraktar [70]. In addition, 3PB tests are simulated for fracture toughness by finite element analysis and the results are compared with the experimental results.

The reinforcements have a different geometry and are distributed randomly in a polymeric composite. As a result, local agglomerations may occur, and the microstructures become very complex. Therefore, the interrelationships between microstructures and the nanoparticles are analyzed with discretized numerical models, which incorporate deformation and damage characteristics particularly on a local scale [70–75]. Homogenization-based multi-scale computational technique is used to observe relationships between microstructures and macro behaviors. The most used homogenization method is representative volume element (RVE) in FEM [70–78]. RVE has been proposed by Nemat-Nasser and Hori [79] and is used in a repeating or periodic nature in the full-scale model. The dependency of the reported results should be verified to the RVE size for composite materials. The RVE includes the microscopic heterogeneities in an averaged sense. The microstructure of the rubber-based composite material can be examined using representative volume elements with different L/R values to verify the stability of the model and the equivalent elastic modulus values of the composite materials can be investigated as future work.

5. Conclusions

Rubber recycling attracts considerable attention by a variety of industries around the world due to shrinking resources, increasing cost of raw materials, growing awareness of sustainable development, and environmental issues. They are commonly used in aeronautic, automotive, and transportation industries. To develop physical and mechanical properties of the recycled rubber, such as fracture toughness and resistance to impact, they are reinforced with microscale particles and there are several studies on design and manufacturing of recycled rubber composites in the literature. Microscale reinforcements (glass bubbles, alumina fiber, etc.) and nanoscale reinforcements (nanosilica, graphene nanoplatelets, etc.) utilized as reinforcements in rubber composites are thoroughly reviewed. In addition, the numerical analysis that can be performed for recycled rubber composites is referred. The general mechanical properties reported by previous studies,

such as tensile, compressive, and flexural strength, are compared with the main goal of demonstrating the amount of reinforcement used. The majority of the studies on recycled rubber composites show that recycled rubber reinforced with microscale particles leads to the development of physical and mechanical properties of the structures and also provides low-cost and lightweight composites for several application areas. Moreover, recycled rubber containing composites can be suitable for applications where high toughness and high resistance to impact are desirable. This study can be useful in terms of providing an idea that recycled rubber composites for use in intermediate and advanced applications can reduce costs in various applications and CO_2 emissions due to their lightweight properties. Consequently, by employing small amounts of reinforcing agent, fewer petrochemical resources are utilized, resulting in environmental sustainability by reducing material prices and energy consumption. Furthermore, the analysis on these types of composites can be improved by several numerical analysis methods. The present review aims to expand the range of the applications of fiber reinforced recycled rubber composites and potential outcomes.

Author Contributions: Conceptualization, E.B.; methodology, G.C.K., O.A., E.B.; software, G.C.K.; validation, E.B., O.A.; formal analysis, E.B., O.A.; investigation, E.B.; resources, E.B.; data curation, G.C.K., E.B., O.A.; writing—original draft preparation, G.C.K.; writing—review and editing, G.C.K., O.A., E.B.; visualization, G.C.K.; supervision, E.B., O.A.; project administration, E.B. and O.A.; funding acquisition, We confirm that there is no Funding. All authors have read and agreed to the published version of the manuscript.

Funding: This research received no external funding.

Conflicts of Interest: The authors declare no conflict of interest.

References

1. Myhre, M.; Saiwari, S.; Dierkes, W.; Noordermeer, J. Rubber recycling: Chemistry, processing, and applications. *Rubber Chem. Technol.* **2012**, *85*, 408–449. [CrossRef]
2. Fukumori, K.; Matsushita, M.; Okamoto, H.; Sato, N.; Suzuki, Y.; Takeuchi, K. Recycling technology of tire rubber. *JSAE Rev.* **2002**, *23*, 259–264. [CrossRef]
3. Zaghloul, M.M.Y.; Mohamed, Y.S.; El-Gamal, H. Fatigue and tensile behaviors of fiber-reinforced thermosetting composites embedded with nanoparticles. *J. Compos. Mater.* **2019**, *53*, 709–718. [CrossRef]
4. Mohamed, Y.S.; El-Gamal, H.; Zaghloul, M.M.Y. Micro-hardness behavior of fiber reinforced thermosetting composites embedded with cellulose nanocrystals. *Alex. Eng. J.* **2018**, *57*, 4113–4119. [CrossRef]
5. Asaro, L.; Gratton, M.; Seghar, S.; Hocine, N.A. Recycling of rubber wastes by devulcanization. *Resour. Conserv. Recycl.* **2018**, *133*, 250–262. [CrossRef]
6. Adhikari, B.; De, D.; Maiti, S. Reclamation and recycling of waste rubber. *Prog. Polym. Sci.* **2000**, *25*, 909–948. [CrossRef]
7. Fang, Y.; Zhan, M.; Wang, Y. The status of recycling of waste rubber. *Mater. Des.* **2001**, *22*, 123–128. [CrossRef]
8. Myhre, M.; MacKillop, D.A. Rubber recycling. *Rubber Chem. Technol.* **2002**, *75*, 429–474. [CrossRef]
9. Mangaraj, D. Rubber recycling by blending with plastics. In *Rubber Recycling*; CRC Press: Boca Raton, FL, USA, 2004; pp. 272–324.
10. Khalil, A.; Shaikh, N.S.; Nudrat, R.Z.; Khalid, M. Effect of micro-sized marble sludge on physical properties of natural rubber composites. *Chem. Indust. Chem. Eng. Quart.* **2013**, *19*, 281–293.
11. Debapriya, D.; Debabish, D. Processing and Material Characteristics of a reclaimed Ground Rubber Tire Reinforced Styrene Butadiene Rubber. *J. Mater. Sci. Appl.* **2011**, *2*, 486–495.
12. Hayeemasae, N.; Ismail, H.; Azura, A.R. Blending of Natural Rubber/Recycled Ethylene- Propylene-Diene Monomer: Cure Behaviors and Mechanical Properties. *Polym. Plast. Technol. Eng.* **2013**, *52*, 501–509. [CrossRef]
13. Ezema, I.C.; Menon, A.R.R.; Obayi, C.S.; Omah, A.D. Effect of Surface Treatment and Fiber Orientation on the Tensile and Morpholoical Properties of Banana Stem Fiber Reinforced Natural Rubber Composite. *J. Miner. Mater. Charact. Eng.* **2014**, *2*, 216–222.
14. Fidelis, C.; Piwai, S.; Benias, N.C.; Upenyu, G.; Mambo, M. Maize Stalk as Reinforcement in Natural Rubber Composites. *Int. J. Sci. Technol. Res.* **2013**, *2*, 263–271.
15. Khaled, F.M.; Rim, H.A.; Gaber, A.I. Feasibility study for end-of-life tire recycling in new tire production, Egypt. *J. Environ. Eng. Ecolog. Sci.* **2014**, *3*, 5.
16. Xiaoou, Z.; Sheng, J.; Xiong, Y.; Xueting, L.; Li, L. Damping acoustic properties of reclaimed rubber/seven-hole hollow polyester fibers composite ma-terials. *J. Comp. Mater.* **2015**, *30*, 48.

17. AL-Nesrawy, S.H.; AL-Maamori, M.; Hassani, A.S.; Jaafar, H.I. Effect of mixture of Reclaimed tire and Carbon Black Percent on the Mechanical properties of SBR/NR blends. *Int. J. Adv. Res.* **2014**, *2*, 234–243.
18. Nabil, H.; Ismail, H.; Azura, A.R. Compounding, mechanical and morphological properties of carbon-black-filled natural rubber/recycled ethylene-propylene-diene-monomer (NR/R-EPDM) blends. *Polym. Test.* **2013**, *32*, 385–393. [CrossRef]
19. Sukanya, S.; Nag, A.; Nando, G.B. Thermoplastic Elastomers from Waste Polyethylene and Reclaim Rubber Blends and Their Composites with Fly Ash. *Process Saf. Environ. Prot.* **2010**, *118*, 131–141.
20. Irene, S.F.; Salahh, M.E.; Hatem, E. Experimental Investigation of Natural Fiber Reinforced Polymers. *Mater. Sci. Appl.* **2012**, *3*, 59–66.
21. Ismail, H.; Edyham, M.R.; Nirjosentono, B. Bamboo fibre filled natural rubber composites: The effects of filler loading and bonding agent. *Polym. Test. B* **2002**, *21*, 139. [CrossRef]
22. Rajan, V.V.; Dierkes, W.K.; Joseph, R.; Noordermeer, J.W.M. Science and technology of rubber reclamation with special attention to NRbased waste latex products. *Progress. Polym. Sci.* **2006**, *31*, 811–834. [CrossRef]
23. Egwaikhide, A.P.; Okieimana, F.E.; Lawal, U. Rheological and Mechanical Properties of Natural Rubber Compounds Filled with Carbonized Palm Kernel Husk and Carbon Black (N330). *Sci. J. Chem.* **2013**, *1*, 50–55.
24. 3M Glass Bubbles K Series, S Series and iM Series. 2021. Available online: http://multimedia.3m.com/mws/media/91049O/3m-glass-bubbles-k-s-and-im-series.pdf (accessed on 25 June 2022).
25. Bhatia, S.; Khan, M.; Sengar, H.; Bhatia, V. A Review on the Mechanical Properties and Environmental Impact of Hollow Glass Microsphere Epoxy Composites. *IIOABJ* **2018**, *9*, 1–8.
26. Gupta, N.; Pinisetty, D.; Shunmugasamy, V.C. *Reinforced Polymer Matrix Syntactic Foams: Effect of Nano and Micro-Scale Reinforcement*; Springer Science & Business Media: Berlin, Germany, 2013.
27. 3M Glass Bubbles. 2021. Available online: https://multimedia.3m.com/mws/media/777234O/3m-glass-bubbles-kunstoffe-article-reprint-2011.pdf (accessed on 25 June 2022).
28. Râpa, M.; Spurcaciu, B.N.; Coman, G.; Nicolae, C.A.; Gabor, R.A.; Ghioca, P.N.; Berbecaru, A.C.; Matei, E.; Predescu, C. Effect of Styrene-Diene Block Copolymers and Glass Bubbles on the Post-Consumer Recycled Polypropylene Properties. *Materials* **2020**, *13*, 543. [CrossRef]
29. Nosker, T.J.; Van Ness, K.E. Fiber orientation and the creation of structural plastic lumber. *Plast. Eng.* **1999**, *55*, 53.
30. Shojaei, A.; Yousefian, H.; Saharkhiz, S. Performance Characterization of Composite Materials Based on Recycled High-Density Polyethylene and Ground Tire Rubber Reinforced with Short Glass Fibers for Structural Applications. *J. Appl. Polym. Sci.* **2007**, *104*, 1–8. [CrossRef]
31. Yu, P.; Manalo, A.; Ferdous, W.; Abousnina, R.; Salih, C.; Heyer, T.; Schubel, P. Investigation on the physical, mechanical and microstructural properties of epoxy polymer matrix with crumb rubber and short fibres for composite railway sleepers. *Constr. Build. Mater.* **2021**, *295*, 123700. [CrossRef]
32. Allouch, M.; Kamoun, M.; Mars, J.; Wali, M.; Dammak, F. Experimental investigation on the mechanical behavior of recycled rubber reinforced polymer composites filled with aluminum powder. *Constr. Build. Mater.* **2020**, *295*, 119845. [CrossRef]
33. Irez, A.B.; Bayraktar, E.; Miskioglu, I. Design and Mechanical-Physical Properties of Epoxy-Rubber Based Composites Reinforced with Nanoparticles. *Procedia Eng.* **2017**, *184*, 486–496. [CrossRef]
34. Irez, A.B. Design, Development and Characterization of Recycled Rubber Modified Epoxy Based Composites: An Experimental Approach for Toughening Mechanisms. Ph.D. Thesis, Université- Paris Saclay, Paris, France, 2018.
35. Irez, A.B.; Bayraktar, E.; Miskioglu, I. Recycled and devulcanized rubber modified epoxy-based composites reinforced with nano-magnetic iron oxide. *Compos. Part B Eng.* **2018**, *148*, 1–13. [CrossRef]
36. Dhingra, A. Alumina fibre fp. *Phil. Trans. R. Soc. Lond. A* **1980**, *294*, 411–417.
37. Madenci, E.; Shkarayev, S.; Mahajan, R. Potential failure sites in a fiip-chip package with and without underfill. *J. Electron. Packag.* **1998**, *120*, 336–341. [CrossRef]
38. Wu, T.; Tsukada, Y.; Chen, W. Materials and mechanics issues in fiip-chip organic packaging. In Proceedings of the 1996 Proceedings 46th Electronic Components and Technology Conference, Orlando, FL, USA, 28–31 May 1996; IEEE: New York, NY, USA, 1996; pp. 524–534.
39. Vo, H.; Todd, M.; Shi, F.; Shapiro, A.; Edwards, M. Towards model-based engineering of underfill materials: CTE modeling. *Microelectron. J.* **2001**, *32*, 331–338. [CrossRef]
40. Craig, R.G. Prosthetic applications of polymers. *Restor. Dent. Mater.* **1997**, *9*, 502–550.
41. Stannard, J.G. *Materials in Dentistry*; Denali Pub: San Francisco, CA, USA, 1988.
42. Babbington, D.; Enos, J.; Cox, J.; Barron, J. Fast-cure vinyl ester meets automotive structural demands. *Mod. Plast. Int.* **1987**, *17*, 106–110.
43. Gong, L.-X.; Zhao, L.; Tang, L.-C.; Liu, H.-Y.; Mai, Y.-W. Balanced electrical, thermal and mechanical properties of epoxy composites filled with chemically reduced graphene oxide and rubber nanoparticles. *Compos. Sci. Technol.* **2015**, *121*, 104–114. [CrossRef]
44. Geim, A.K.; Novoselov, K.S. The rise of graphene. *Nat. Mater.* **2007**, *6*, 183. [CrossRef] [PubMed]
45. Wichmann, M.H.; Schulte, K.; Wagner, H.D. On nanocomposite toughness. *Compos. Sci. Technol.* **2008**, *68*, 329–331. [CrossRef]

46. Liang, Y.; Pearson, R. Toughening mechanisms in epoxy-silica nanocomposites (ESNs). *Polymer* **2009**, *50*, 4895–4905. [CrossRef]
47. Srivastava, I.; Koratkar, N. Fatigue and fracture toughness of epoxy nanocomposites. *JOM* **2010**, *62*, 50–57. [CrossRef]
48. Balandin, A.A.; Ghosh, S.; Bao, W.; Calizo, I.; Teweldebrhan, D.; Miao, F.; Lau, C.N. Superior thermal conductivity of single-layer graphene. *Nano Lett.* **2008**, *8*, 902–907. [CrossRef] [PubMed]
49. Scarpa, F.; Adhikari, S.; Phani, A.S. Effective elastic mechanical properties of single layer graphene sheets. *Nanotechnology* **2009**, *20*, 065709. [CrossRef] [PubMed]
50. Mittal, G.; Dhand, V.; Rhee, K.Y.; Park, S.-J.; Lee, W.R. A review on carbon nanotubes and graphene as fillers in reinforced polymer nanocomposites. *J. Ind. Eng. Chem.* **2015**, *21*, 11–25. [CrossRef]
51. Irez, A.B.; Bayraktar, E.; Miskioglu, I. Fracture Toughness Analysis of Epoxy-Recycled Rubber-Based Composite Reinforced with Graphene Nanoplatelets for Structural Applications in Automotive and Aeronautics. *Polymers* **2020**, *12*, 448. [CrossRef] [PubMed]
52. Irez, A.B.; Zambelis, G.; Bayraktar, E. A New Design of Recycled Ethylene Propylene Diene Monomer Rubber Modified Epoxy Based Composites Reinforced with Alumina Fiber: Fracture Behavior and Damage Analyses. *Materials* **2019**, *12*, 2729. [CrossRef] [PubMed]
53. Irez, A.B.; Bayraktar, E.; Miskioglu, I. Flexural fatigue damage analyses of recycled rubber-modified epoxy-based composites reinforced with alumina fibres. *Fatigue Fract. Eng. Mater. Struct.* **2019**, *42*, 959–971. [CrossRef]
54. Irez, A.B.; Bayraktar, E.; Miskioglu, I. *Toughening Mechanism in Epoxy Resin Modified Recycled Rubber Based Composites Reinforced with Gamma-Alumina, Graphene and CNT*; The Society for Experimental Mechanics, Inc.: Bethel, CT, USA, 2019; Volume 5, pp. 31–39.
55. Zaghloul, M.M.Y.; Zaghloul, M.Y.M.; Zaghloul, M.M.Y. Experimental and modeling analysis of mechanical-electrical behaviors of polypropylene composites filled with graphite and MWCNT fillers. *Polym. Test.* **2017**, *63*, 467–474. [CrossRef]
56. Zaghloul, M. Mechanical properties of linear low-density polyethylene fire-retarded with melamine polyphosphate. *J. Appl. Polym. Sci.* **2018**, *135*, 46770. [CrossRef]
57. Keledi, G.; Sudár, A.; Burgstaller, C.; Renner, K.; Móczó, J.; Pukánszky, B. Tensile and impact properties of three-component PP/wood/elastomer composites. *Express Polym. Lett.* **2012**, *6*, 224–236. [CrossRef]
58. Jose, J.; Nag, A.; Nando, G.B. Processing and characterization of recycled polypropylene and acrylonitrile butadiene rubber blends. *J. Polym. Environ.* **2010**, *18*, 155–166. [CrossRef]
59. Panaitescu, D.M.; Vuluga, Z.; Sanporean, C.G.; Nicolae, C.A.; Gabor, R.; Trusca, R. High flow polypropylene/SEBS composites reinforced with differently treated hemp fibers for injection molded parts. *Compos. B Eng.* **2019**, *174*, 107062. [CrossRef]
60. Amos, S.E.; Yalcin, B. *Hollow Glass Microspheres for Plastics, Elastomers, and Adhesives Compounds*; Elsevier: Amsterdam, The Netherlands, 2015.
61. Râpa, M.; Matei, E.; Ghioca, P.N.; Grosu, E.; Iancu, L.; Spurcaciu, B.; Trifoi, A.R.; Gherman, T.; Pica, A.; Predescu, A.M.; et al. Improvement of some post-consumer polypropylene (rPP) by melt modification with styrene-diene block copolymers. *EEMJ* **2017**, *16*, 2615–2624.
62. Zaghloul, M.M.Y.; Zaghloul, M.Y.M.; Zaghloul, M.M.Y. Developments in polyester composite materials, An in-depth review on natural fibres and nano fillers. *Compos. Struct.* **2021**, *278*, 114698. [CrossRef]
63. Yalcın, D.; Balcıoglu, H.; Akta, M. Tamir Edilmi^3 Dogal Lif Takviyeli Kompozitlerin Mekanik Dayanimlari. In Proceedings of the Third International Aegean Composite Materials Symposium, Kusadasi, Turkey, 5–7 November 2015; pp. 544–552.
64. Donald, R.A. *Essentials of Materials Science and Engineering*, SI ed.; Cengage Learning: Boston, MA, USA, 2018; p. 211.
65. Askeland, D.R.; Wright, W.J. *Science and Engineering of Materials*; Nelson Education: Toronto, ON, Canada, 2015.
66. Her, S.C.; Liu, S.J. Analytical model for predicting the interfacial stresses of carbon nanotubes-reinforced nanocomposites. *Eng. Comput.* **2014**, *31*, 353–364. [CrossRef]
67. Halpin, J.C.; Kardos, J.L. The Halpin-Tsai equations: A review. *Polym. Eng. Sci.* **1976**, *16*, 344–352.
68. Armbrister, C.E.; Okoli, O.I.; Shanbhag, S. Micromechanics predictions for two-phased nanocomposites and three-phased multiscale composites: A review. *J. Reinf. Plast. Compos.* **2015**, *34*, 605–623. [CrossRef]
69. Takayanagi, M.; Uemura, S.; Minami, S. Application of equivalent model method to dynamic rheo-optical properties of crystalline polymer. *J. Polym. Sci. C Polym. Symp.* **1964**, *5*, 113–122. [CrossRef]
70. Kabakci, G.C.; Aslan, O.; Bayraktar, E. Toughening Mechanism Analysis of Recycled Rubber-Based Composites Reinforced with Glass Bubbles, Glass Fibers and Alumina Fibers. *Polymers* **2021**, *13*, 4215. [CrossRef] [PubMed]
71. Odegard, G.M.; Gates, T.S.; Wise, K.E.; Park, C.; Siochi, E.J. Constitutive modeling of nanotube–reinforced polymer composites. *Compos. Sci. Technol.* **2003**, *63*, 1671–1687. [CrossRef]
72. Odegard, G.M.; Pipes, R.B.; Hubert, P. Comparison of two models of SWCN polymer composites. *Compos. Sci. Technol.* **2003**, *64*, 1011–1020. [CrossRef]
73. Zeng, Q.H.; Yu, A.B.; Lu, G.Q. Multiscale modeling and simulation of polymer nanocomposites. *Prog. Polym. Sci.* **2008**, *33*, 191–269. [CrossRef]
74. Peng, R.D.; Zhou, H.W.; Wang, H.W.; Mishnaevsky, L., Jr. Modeling of nano-reinforced polymer composites: Microstructure effect on Young's modulus. *Comput. Mater. Sci.* **2012**, *60*, 19–31. [CrossRef]
75. Wang, H.W.; Zhou, H.W.; Peng, R.D.; Mishnaevsky, L., Jr. Nanoreinforced polymer composites: 3D FEM modeling with effective interface concept. *Compos. Sci. Technol.* **2011**, *71*, 980–988. [CrossRef]

76. Li, Y.; Waas, A.M.; Arruda, E.M. A closed-form, hierarchical, multi-interphase model for composites—Derivation, verification and application to nanocomposites. *J. Mech. Phys. Solids* **2011**, *59*, 43–63. [CrossRef]
77. Mortazavi, B.; Bardon, J.; Ahzi, S. Interphase effect on the elastic and thermal conductivity response of polymer nanocomposite materials: 3D finite element study. *Comput. Mater. Sci.* **2013**, *69*, 100–106. [CrossRef]
78. Sun, C.T.; Vaidya, R.S. Prediction of composite properties from a representative volume element. *Compos. Sci. Technol.* **1996**, *56*, 171–179. [CrossRef]
79. Nemat-Nasser, S.; Hori, M. *Micromechanics: Overall Properties of Heterogeneous Materials*; North-Holland Publishing Company: Amsterdam, The Netherlands, 1999.